Theoretical calculations of electron transport in molecular junctions: Inflection behavior in Fowler-Nordheim plot and its origin

Masaaki Araidai* and Masaru Tsukada†

WPI Advanced Institute for Materials Research, Tohoku University, 2-1-1 Katahira, Aoba-ku, Sendai, Miyagi 980-8577, Japan and CREST, Japan Science and Technology Agency, 4-1-8 Honcho Kawaguchi, Saitama 332-0012, Japan

(Received 24 November 2009; revised manuscript received 9 February 2010; published 15 June 2010)

We investigated the origin of an inflection behavior appearing in Fowler-Nordheim (F-N) plot of current-voltage characteristics for molecular junctions using two different levels of calculation methods: nonequilibrium Green's-function technique combined with the density-functional theory and tight-binding approximation. Although the inflection has so far been interpreted from the naive model that the charge transport mechanism transits from a direct to the F-N tunneling, our results indicated that the inflection does not necessarily mean the transition between the two regimes. We found from the close examination of the relation between the behavior of the F-N curve and the transmission function that the inflection takes place when the molecular level responsible for electric currents approaches to the edge of the bias window. While our interpretation for the inflection drastically differ from the conventional model, the F-N plots obtained from our calculations showed closely similar behavior as those from the recent experiments.

DOI: 10.1103/PhysRevB.81.235114 PACS number(s): 73.63.−b, 73.40.Gk, 72.10.−d, 85.65.+h

I. INTRODUCTION

Current-voltage characteristics of diverse kinds of molecular junctions generally exhibit nonlinear behaviors that are explicitly characterized as an inflection in Fowler-Nordheim (F-N) plot.[1–4] The inflection of the F-N curve has so far been qualitatively understood by a simple barrier picture.[2,5] Although this barrier description is known to be deficient in capturing quantitative aspects of tunneling through molecules, the interpretation has been accepted because it allows us to understand in a straightforward manner the cause of the inflection observed in experiments. According to the simple model, at the zero-bias limit the shape of the tunneling barrier is rectangular, and the expression of currents is described as

$$I \propto V \exp\left[-\frac{2d\sqrt{2m\phi}}{\hbar}\right], \tag{1}$$

where V is the applied bias voltage, d is the barrier width, m is the electron effective mass, and ϕ is the barrier height. Then, $\ln(I/V^2)$ is proportional to $\ln(1/V)$. At the opposite limit where the tunneling barrier becomes triangular, the current-voltage dependence is

$$I \propto V^2 \exp\left[-\frac{4d\sqrt{2m\phi^3}}{3\hbar qV}\right], \tag{2}$$

resulting in $\ln(I/V^2) \propto -1/V$. In the above, q is the electronic charge. Tunneling in the high-voltage regime shows the feature of a field emission or F-N tunneling. The overall behavior of the F-N curve with respect to applied bias voltage is shown in Fig. 1, together with the conventional barrier picture. On the basis of the above interpretation, the inflection in the F-N plot has so far been believed to be the evidence that the charge transport mechanism transits from a direct to F-N tunneling.[2,4]

Recently, Beebe *et al.* has proposed an intriguing experimental technique, transition voltage spectroscopy (TVS).[2,4] The transition voltage means the voltage at which the transition as stated above occurs. Toward deep understandings of charge transport mechanisms through molecules, TVS may become a powerful tool to probe the energy offset between the metal Fermi energy and the closest molecular levels.

While the experimental behaviors can be successfully explained by the naive barrier picture, the concept of the transition remains unclear. The barrier picture works well as long as the effective-mass approximation remains valid at the Fermi level. However, many organic molecular junctions display large insulating gaps and flat bands, and the effective-mass approximation for these systems often fails when one moves away from the band edges. In contrast, the modern theory beyond the effective-mass treatments has been successfully applied to clarify the microscopic mechanisms of tunneling transport of molecular junctions, especially length dependence of off-resonant tunneling[6–9] and current-voltage characteristics.[6,10–12] The former has been well understood from the complex-band structure on monomer units in sandwiched molecular chains,[7–9] which is directly connected with the evanescent states in the molecule. In the latter case, the position of resonant states originating from molecular high-

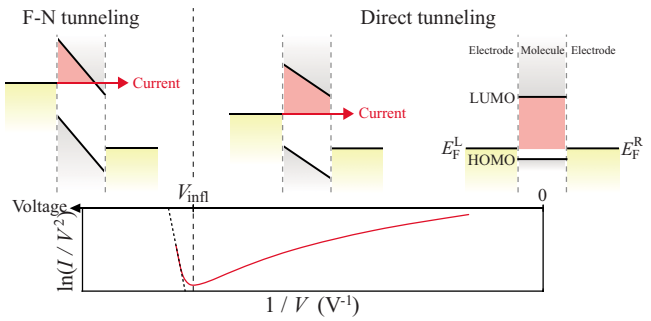

FIG. 1. (Color online) Schematic of the conventional model to qualitatively explain the inflection of F-N curve. E_F^L and E_F^R are the Fermi energies of both electrodes and V_{infl} is the voltage at which the inflection takes place. The darker-shaded (red) area (triangle, trapezoidal, or rectangle in the upper panel) represents the tunneling barrier.

est occupied molecular orbital (HOMO) or lowest unoccupied molecular orbital (LUMO) levels against the metal Fermi energy is one of the key factors to determine the value of electric currents, and their information should be intrinsically captured by the TVS measurements. The most important thing in both analyses is the molecular nature that cannot be described by the naive barrier picture. Accordingly, theoretical calculations by the modern theory is essential for investigating whether the inflection of the F-N curve means the transition from the direct to F-N tunneling, from the viewpoints not of tunneling barrier but resonant tunneling.

The outline of this paper is as follows. The calculation methods and models used here are described in Sec. II. We perform two different levels of calculations: density-functional theory (DFT) (Ref. 13) with realistic atomic configurations and tight-binding (TB) approximation with simple atomic chain structures for molecules. In Sec. III, we present numerical results for the F-N plots by the DFT and TB calculations. We focus only on the generation mechanism of the inflection, not on the length dependence. All the results show that the existence of the turning point in the F-N plot does not necessarily mean the transition between the direct and F-N tunneling. We further discuss the cause of the inflection, and the similarity and difference between the naive barrier picture and the resonant-tail model confirmed by the present calculation. Section IV is devoted to a summary of this paper.

II. METHOD AND MODEL

Tunneling currents through molecules were calculated by the nonequilibrium Green's-function (NEGF) technique.[14] This method is more general treatment than the pioneering theory by Mujica and Ratner[6] because the NEGF scheme is applicable to arbitrarily large bias cases. We employed the NEGF technique to calculate current-voltage characteristics of molecular junctions.[14] The premise of this method is to divide the system into three regions: the left and right electrodes in thermal equilibrium and the central scattering region. The Green's function of the scattering region includes the self-energy generated by the electrodes $\boldsymbol{\Sigma}_{\mathrm{L/R}}$,

$$\boldsymbol{G}(E) = \{E\boldsymbol{S} - [\boldsymbol{H} + \boldsymbol{\Sigma}_{\mathrm{L}}(E) + \boldsymbol{\Sigma}_{\mathrm{R}}(E)]\}^{-1}, \tag{3}$$

where $\boldsymbol{H}$ and $\boldsymbol{S}$ are the Hamiltonian and overlap matrices, respectively. Then, the expression of the transmission function and electric current for applied bias V are

$$T(E,V) = 4\ \mathrm{Tr}[\mathrm{Im}(\boldsymbol{\Sigma}_{\mathrm{L}})\boldsymbol{G}^{\dagger}\ \mathrm{Im}(\boldsymbol{\Sigma}_{\mathrm{R}})\boldsymbol{G}], \tag{4}$$

$$I(V) = G_0 \int_{-\infty}^{+\infty} T(E,V)[f(E-E_{\mathrm{F}}^{\mathrm{L}}) - f(E-E_{\mathrm{F}}^{\mathrm{R}})]dE, \tag{5}$$

where $G_0 = 2e^2/h$, $E_{\mathrm{F}}^{\mathrm{L}}$ and $E_{\mathrm{F}}^{\mathrm{R}}$ are the Fermi energies of both electrodes, and f is the Fermi-Dirac distribution function. In off-resonant tunneling, the above Green's function shows the decaying behavior similar to the evanescent states in the molecule, resulting in the exponential decay feature of conductance with the molecular length. The feature has been expressed explicitly within the linear-response regime[6] and the complex-band analysis.[7–9]

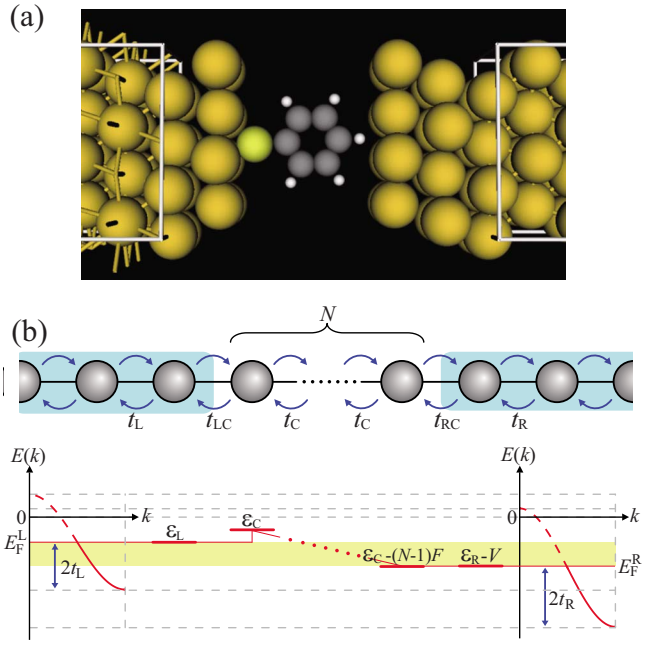

FIG. 2. (Color online) (a) The Ph-SH sandwiched between gold (111) surfaces is depicted as a model for *ab initio* calculations. White boxes denote the electrode regions. (b) The atomic configuration and energy diagram for tight-binding calculations are shown in the upper and lower panels, respectively. The onsite energy and hopping integral are represented by ε and t, in which the subscripts C, L, and R mean the central scattering region, the left, and right electrodes, respectively. N is the number of atoms in the central region and F is a virtual field which is defined by $V/(N-1)$. The shaded areas in the upper and lower panels show the electrode regions and the bias window, respectively.

We utilized two different levels of methods, DFT and TB calculations, as a means to extract some physical quantities and matrices necessary for the NEGF scheme. The NEGF+DFT (*ab initio*) calculation[15,16] is the most sophisticated method to perform the numerical analysis of open systems under nonequilibrium conditions. We used the commercially available Atomistix ToolKit (ATK).[17] This code employs numerical atomic orbitals and norm-conserving pseudopotentials.[18] We used single-zeta orbitals with polarization and the local-density approximation for the exchange-correlation potential.[19] A phenyl-thiol (Ph-SH) molecule sandwiched between gold (111) electrodes shown in Fig. 2(a) was adopted as a model for the *ab initio* calculations. In the NEGF+TB calculations, for simplicity, we employed a straight chain structure of atoms given in Fig. 2(b). The energy diagram is also depicted in Fig. 2(b). The quantity F is a virtual field responsible for the energy shift of molecular levels, which is implicitly included in the *ab initio* calculations through the electrostatic potential.

In the following section, we first present the F-N plot obtained from the *ab initio* calculations for Ph-SH and reveal the *I-V* behaviors using the transmission functions. Next, the results of the TB calculations for the atomic chain are shown to gain the further understanding of the origin of the inflection in the F-N plot. For our goal, we consider two model cases of atomic chains, whose energy diagrams are given in

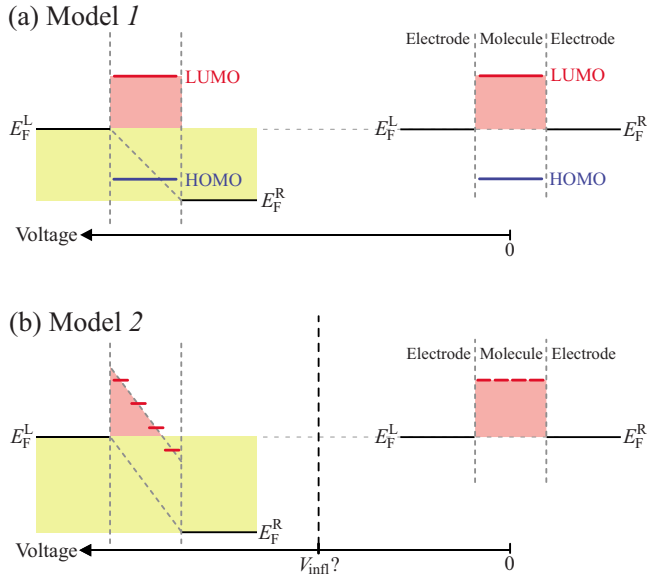

FIG. 3. (Color online) Energy diagrams for models 1 and 2 in the tight-binding calculations are given in (a) and (b), respectively. The darker-shaded (red) area represents the tunneling barrier from the conventional model. In the model 1, molecular levels are delocalized over the central region owing to the strong coupling between the atoms and the electric field is not applied. On the other hand, molecular levels of the model 2 are localized around the atoms (molecules) owing to the weak coupling and show the constant gradient due to the electric field.

Figs. 3(a) and 3(b), respectively. The model 1 corresponds to the case of single-molecular junctions, but without electric field, namely, *no* level shifts. The molecular orbitals are spread over the central region owing to the strong coupling between the atoms. According to the conventional model, the inflection should *not* take place because the shape of the tunneling barrier is always rectangular owing to the fixed levels. On the other hand, the model 2 is created so that the spatial distribution of the tunnel barriers mimics the conventional triangular barrier model in Fig. 1. In this model, we assume a molecular chain with a single level per molecule. The coupling energy between the molecules is assumed to be much smaller than those among the atoms in the same molecule. Accordingly, the molecular levels are localized around each molecule. Applying the bias voltage, the field is assumed to come into the molecular chain, resulting in a gradient in the distribution of the levels due to the electric field, as depicted in Fig. 3(b), and the shape of the tunneling barrier becomes triangular at higher biases. Therefore, the model 2 is somewhat similar to the conventional model stated in Sec. I. In Sec. III C, the similarity is confirmed from the energy diagram and the local density of states (LDOS). The numerical values of the parameters for the tight-binding calculations are summarized in Table I.

TABLE I. Numerical parameters for the tight-binding calculations given in the caption of Fig. 2. $\varepsilon_L=\varepsilon_R=0.0$, $t_L=t_R=1.0$, $t_{LC}=0.2$, and $t_{RC}=0.02$ in units of electron volt.

	ε_C	t_C	V_b	Field
Model 1	0.00	0.25	0.0–0.25	OFF
Model 2	0.50	0.025	0.0–0.50	ON

III. RESULT AND DISCUSSION

A. *Ab initio* results

Figure 4 shows the F-N plot of the current-voltage characteristic and transmission function of Ph-SH by the *ab initio* calculations. We immediately find from Fig. 4(a) that the calculated F-N curve shows the similar behavior as the recent experiments,[2–4] in which the behavior after the inflection is almost linear. The voltage at which the inflection of the F-N curve takes place, V_{infl}, is 0.32 V.[20] In order to clarify the behavior of the F-N curve, we closely examine the transmission function given in Fig. 4(b). The peaks correspond to the HOMO levels at different bias voltages. The longer dotted bar is the bias window at 0.4 V and the shorter one at 0.3 V. The HOMO peak at 0.3 V is outside the bias window and the peak at 0.4 V is inside the bias window. Consequently, the behavior of the F-N curve is apparently explained by the interpretation that the entering of the HOMO peak into the bias window at 0.32 V sharply enhance the magnitude of electric current, resulting in the inflection. However, the inflection seems to take place somewhat before the resonant peak gets into the bias window.

To clearly see the relation between the inflection voltage V_{infl} and the spectral shape of the transmission function, we

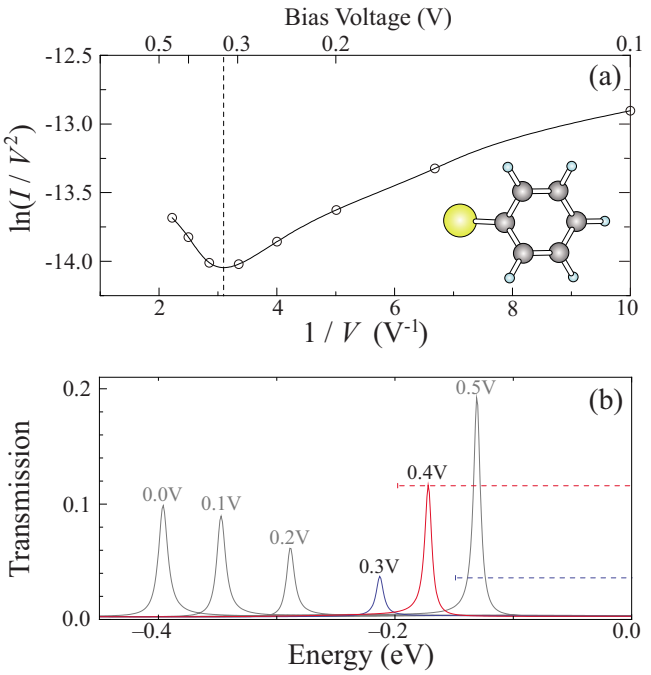

FIG. 4. (Color online) Results obtained from the *ab initio* calculations of Ph-SH. (a) and (b) are the F-N plot of the current-voltage characteristics and the transmission function around the HOMO level at each bias voltage. The solid line in (a) is a guide for the eyes. In (b), the origin of energy is set to the averaged value of the Fermi energies between the left and right electrodes, and the longer dotted bar is the bias window at 0.4 V and the shorter one is that at 0.3 V.

consider the Lorentzian and Gaussian functions as the shape,

$$T(E) = \begin{cases} T_{\text{peak}} \dfrac{(\Gamma/2)^2}{(E - E_{\text{peak}})^2 + (\Gamma/2)^2} \\ T_{\text{peak}} \exp\left[- \dfrac{(E - E_{\text{peak}})^2}{2\sigma^2} \right] \end{cases}, \quad (6)$$

where T_{peak} is the height of the peak and E_{peak} is the center position. We assumed the values of these parameters as $T_{\text{peak}}=0.01$ and $E_{\text{peak}}=-1.0$ eV. The width of the Gaussian function is controlled by σ which is related to the full width at half maximum Γ according to $\Gamma=2\sqrt{2 \ln 2}\sigma$. The value of electric currents is defined by the integral from the given bias to the origin.

The transmission functions and the corresponding F-N plots with various Γ are shown in Figs. 5(a) and 5(b), respectively. We definitely observe in Fig. 5(b) that every F-N curve possesses a turning point. The inflection voltages of the Lorentzian and Gaussian, $V_{\text{infl}}^{\text{L}}$ and $V_{\text{infl}}^{\text{G}}$, with $\Gamma=0.2$ are 0.50 and 0.012 V, which are represented by the vertical solid and broken lines in Fig. 5. The $V_{\text{infl}}^{\text{L/G}}$ with minus sign in Fig. 5(a) means the lower limit of the bias window. Accordingly, we find that the inflection takes place when a certain amount of the tail of the resonant peak enters the window. In addition, the $V_{\text{infl}}^{\text{L}}$ is much larger than the $V_{\text{infl}}^{\text{G}}$ while the $V_{\text{infl}}^{\text{L}}$ is almost the same value even if the Γ is different. This means that the value of V_{infl} strongly depends on the slope of the tail which directly affects the increasing rate of electric currents. Furthermore, considering that the transmission shape is generally Lorentzian, the fact that there is little difference of V_{infl} even if the Γ is different implies that V_{infl} values are insensitive to the experimental setup.[2,4]

To understand the similarity and difference between the present results and the naive conventional barrier model shown in Fig. 1, the effective potential of electrons for the present molecular junction calculated by the *ab initio* method are presented in Fig. 6(a) for the zero-bias case and in Fig. 6(b) at 0.4 V on the right electrode. The solid curves in Fig. 6 are the potentials averaged over the plane parallel to the substrate surface. Notice that the significant difference between the two potentials cannot be found, though the bias voltage 0.4 V is above the inflection voltage. Different from the conventional model, the microscopic potential in the molecule shows a strongly corrugated feature; the deep valleys correspond to the atomic planes and the sharp ridges

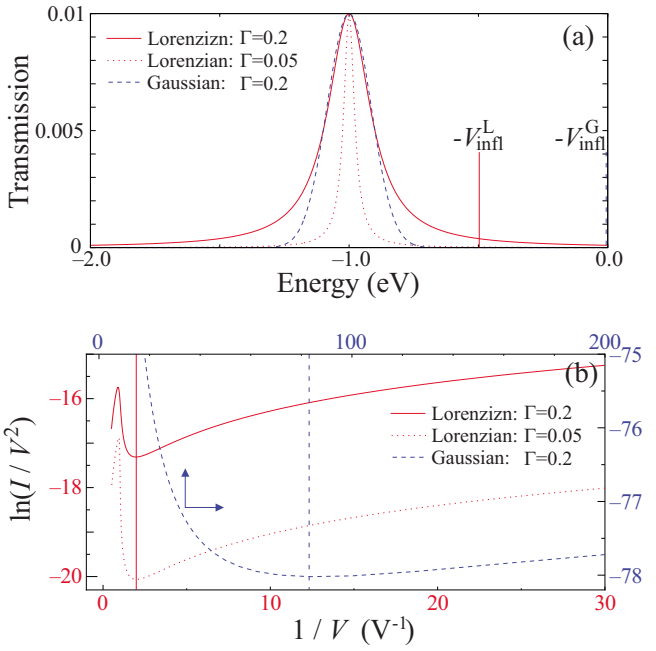

FIG. 5. (Color online) (a) Transmission functions which we assume as the model of resonant peak. (b) F-N plots for the crude models. The left and lower axes in (b) are for the Lorentzian cases (solid and dotted curves) and the right and upper axes in (b) for the Gaussian case (dashed curve). The vertical solid and broken lines in (a) and (b) indicate the inflection voltages in the Lorentzian and the Gaussian cases with $\Gamma=0.2$.

correspond to the interatomic bonds. Electrons in the molecule feel such corrugated potential and due to the multireflection and interference of the scattering waves, the allowed electron energies tend to be bunched into narrow resonant levels attributed to the molecular levels in the isolated state. Note that the width of the resonance is finite though narrow since electrons can tunnel out of the molecule through the outermost potential barrier into the substrate or vice versa. When the resonant level associated with the HOMO (or LUMO) level is located enough below (above) the Fermi levels, the rate of the electron transfer across the boundaries between the molecule and the substrate is very small because it is caused by the tiny tail of the resonant level. With the increase in the bias voltage, it approaches to the bias window, leading to a gradual slow increase in the electric current. This feature successfully explains the *I-V* curve in the

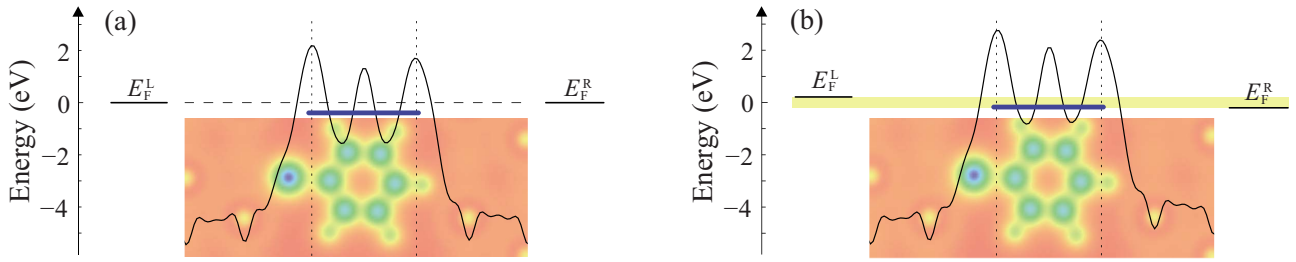

FIG. 6. (Color online) Effective potentials of electrons around Ph-SH at (a) 0.0 and (b) 0.4 V. The solid curves are the potentials averaged over the plane normal to the substrate. The insets show spatial distributions of the effective potentials on the plane across the center of sulfur. Thick gray (blue) bars indicate the peak positions of the HOMO levels.

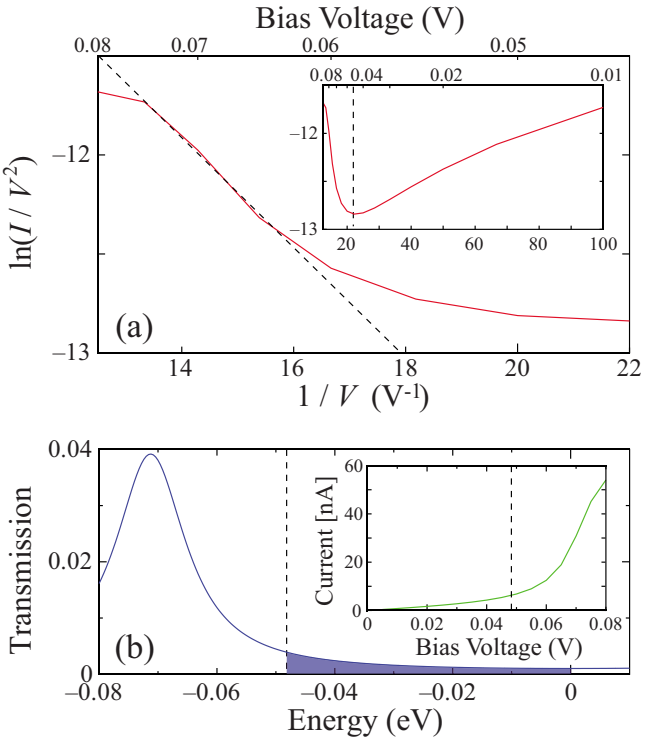

FIG. 7. (Color online) (a) F-N plot and (b) transmission function around the HOMO peak for the model 1 with $N=10$. The insets in (a) and (b) indicate the global behavior of the F-N curve and the current-voltage curve, respectively. The vertical dashed lines in both insets denote the inflection voltage V_{infl}, and the vertical line in the main figure of (b) represents the lower limit of the bias window at V_{infl}. The shaded area means the magnitude of electric current at V_{infl}.

smaller bias region than the inflection voltage. From the viewpoint that the tunneling rate is determined by the tail of the allowed states, the above mechanism of the tunnel current in the present system is similar to the "direct tunneling" in the conventional barrier model. However, in the conventional model, the allowed states are the continuum states existing above such kind of the barrier. Considering the fact that such a simple "rectangular or triangular barrier" is absent in the molecular region and the tail of the resonance in the present system is associated with not the continuum states but the discrete molecular levels, the conventional model is not adequate as a model of tunnel mechanisms of molecular junctions. When the resonant level associated with HOMO (LUMO) approaches very much to the lower (upper) edge of the bias window, the increase in the current with the bias becomes significantly steep, showing the precursor of the resonant peak of the transmission function. As explained above, this results in the inflection behavior of the F-N curve. However, this mechanism for the inflection behavior is completely different from the transition from the direct to F-N tunneling in the conventional model.

The most important finding in this section (and in the present study) is that the inflection of the F-N curve takes place when the *tail* of the resonant peak enters the bias window. We further investigate the mechanism of the inflection, and the similarity and difference between the conventional and our models, through two model calculations in the following subsections.

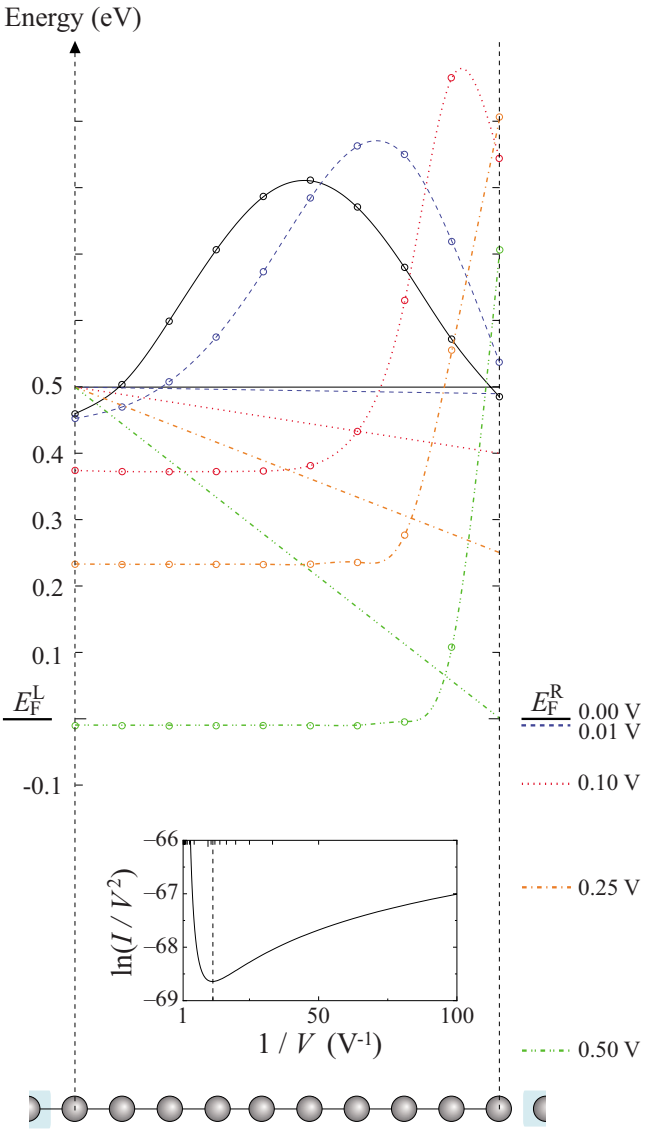

FIG. 8. (Color online) Energy diagram for the model 2, together with LDOS in arbitrary units at 0.00 (solid), 0.01 (dashed), 0.10 (dotted), 0.25 (dotted-dashed), and 0.50 V (two dotted-dashed). Each LDOS curve is drawn with shift of the origin and the left edge of the curve is set to the energy of peak center of the lowest molecular level responsible for the electric current in this model. The straight lines show the gradients due to the electric fields which may correspond to the tunnel barrier in the conventional model. The inset represents the F-N plot.

B. Tight-binding results: Model 1

We present the TB results of the model 1. Note again that the model 1 was created so that according to the view based on the conventional model the turning point *cannot* exist in the F-N plot. We focus on the model with $N=10$ because the results with different numbers are qualitatively the same.

The F-N plot is shown in Fig. 7(a). The global behavior of the F-N curve given in the inset shows the similar behavior

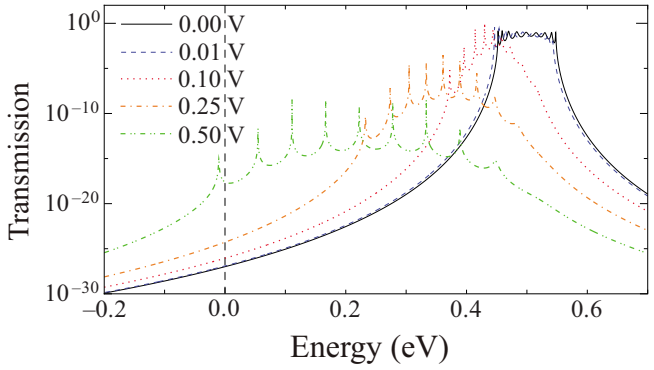

FIG. 9. (Color online) Transmission function at each bias voltage for the model 2. The vertical dashed line denotes the upper limit of the bias window (0 V). The lower limit is $-V$.

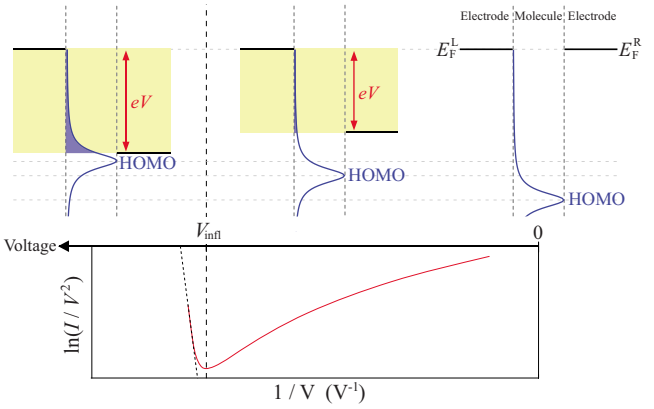

FIG. 10. (Color online) Our scenario for the inflection of the F-N curve.

as the recent experiments[2–4] and also the *ab initio* calculations mentioned before. The local behavior after the inflection in the main figure looks like linear even if the calculation is not based on the simple barrier picture. The transmission function around the HOMO peak is represented in Fig. 7(b), in which the inset is the current-voltage curve. Here, the HOMO level means the molecular level which has a smaller energy than the Fermi energies of both electrodes and is the closest to the Fermi energies at the zero bias. The vertical dashed lines in the main figure and the inset denote the lower limit of the bias window ($-V_{\mathrm{infl}}$ in this case) and the inflection voltage V_{infl}, respectively. The shaded area is the amount of electric current. It is found from Fig. 7(b) that the inflection takes place before the resonant peak gets into the bias window, as in the previous section. While these features of the model 1 cannot be explained by the conventional model, they can be consistently explained by our interpretation.

C. Tight-binding results: Model 2

The TB results of the model 2 with $N=10$ are presented in this section. By construction, the model 2 may be similar to the conventional model. In this case, the bias window is defined by the interval between the origin and $-V$.

Figure 8 shows the energy diagram of this model together with the LDOS at the energy of the center position of the resonant peak originating from the lowest molecular level at each bias voltage (main figure) and the F-N plot (inset) in which the vertical broken line is the inflection voltage $V_{\mathrm{infl}}=0.085$ V. The gradient depicted by the straight line in the main figure represents not only the electric field at the bias but also the distribution of the molecular levels which mimics the spatial distribution of the tunnel barriers. The transmission functions given in Fig. 9 are also used to closely examine the relation between the behavior of the F-N curve and the molecular levels.

We observe from Fig. 8 that with the increase in applied bias, the LDOS peak steadily moves toward the positive electrode and the lowest molecular level shifts toward the lower side of energy. The latter is explicitly found also from Fig. 9. These features imply that the approach of the lowest level to the bias window strongly enhances the probability of the electron tunneling from the left electrode through the molecules toward the right electrode. This means that the tunneling mechanism in this model is somewhat similar to the conventional model. However, there is a large difference of V_{infl} between our and the conventional model. While the value of V_{infl} is speculated by the conventional model to be 0.5 V, our V_{infl} is 0.085 V. Further, we explicitly find from the F-N plot in the inset of Fig. 8 and the transmission functions in Fig. 9 that the turning point appears rather before the lowest level approaches to the upper limit of the bias window. Therefore, in this case, the inflection seems to take place in the "direct tunneling regime." Although there are some similarities and differences between both models, ours is also able to explain the experimental behaviors very well.

IV. SUMMARY

The origin of the inflection in the F-N plot of current-voltage characteristics for molecular junctions was investigated by two different levels of methods: NEGF+DFT and TB calculations. The experimental behaviors of the F-N curve were well reproduced by all the calculations including the discrete levels in the molecular region. From a naive consideration, it is not trivial whether such models show the inflection behavior. Even if we naively assumed that the transmission function of the resonant peak responsible for electric currents has a spectral shape of either Lorentzian or Gaussian functions, the inflection behavior of the F-N curve was reproduced clearly. This seems to imply that the inflection on the F-N plot is one of the general features in the integration of the bell-shaped function. The close examinations of the relation between the behavior and the transmission function demonstrated that the inflection takes place when a certain amount of the tail of the resonant peak gets into the bias window. Our scenario for the inflection is schematically summarized in Fig. 10. In this study, we referred to the electron transport originating only from the HOMO level. However, if the bias is inverted, the same conclusions for the LUMO level should be realized.

Although the inflection has so far been interpreted from the conventional model that the charge transport mechanism

transits from a direct to the F-N tunneling,[2,4] our results indicated that it does not necessarily mean the transition between the two regime. While our interpretation of the inflection drastically differs from the conventional model, the experimental behaviors can be rationalized by our resonant-tail picture.

ACKNOWLEDGMENTS

This research was supported by a Grant-in-Aid for Scientific Research on Priority Areas "Electron transport through a linked molecule in nano-scale" from the Ministry of Education, Culture, Sports, Science and Technology of Japan.

*araidai@wpi-aimr.tohoku.ac.jp
†tsukada@wpi-aimr.tohoku.ac.jp

[1] *Introducing Molecular Electronics*, Lecture Notes in Physics Vol. 680, edited by G. Cuniberti, G. Fagas, and K. Richter (Springer, Berlin, 2005).
[2] J. M. Beebe, B.-S. Kim, J. W. Gadzuk, C. D. Frisbie, and J. G. Kushmerick, Phys. Rev. Lett. **97**, 026801 (2006).
[3] Y. Noguchi, T. Nagase, R. Ueda, T. Kamikado, T. Kubota, and S. Mashiko, Jpn. J. Appl. Phys. **46**, 2683 (2007).
[4] J. M. Beebe, B.-S. Kim, C. D. Frisbie, and J. G. Kushmerick, ACS Nano **2**, 827 (2008).
[5] J. G. Simmons, J. Appl. Phys. **34**, 1793 (1963).
[6] V. Mujica and M. A. Ratner, Chem. Phys. **264**, 365 (2001).
[7] J. K. Tomfohr and O. F. Sankey, Phys. Rev. B **65**, 245105 (2002).
[8] G. Fagas, A. Kambili, and M. Elstner, Chem. Phys. Lett. **389**, 268 (2004).
[9] S. Y. Quek, H. J. Choi, S. G. Louie, and J. B. Neaton, Nano Lett. **9**, 3949 (2009).
[10] K. Tagami, M. Tsukada, T. Matsumoto, and T. Kawai, Phys. Rev. B **67**, 245324 (2003).
[11] J. Taylor, M. Brandbyge, and K. Stokbro, Phys. Rev. B **68**, 121101(R) (2003).
[12] D. Q. Andrews, R. Cohen, R. P. Van Duyne, and M. A. Ratner, J. Chem. Phys. **125**, 174718 (2006).
[13] W. Kohn, Rev. Mod. Phys. **71**, 1253 (1999).
[14] S. Datta, *Electronic Transport in Mesoscopic Systems* (Cambridge University Press, New York, 1995).
[15] J. Taylor, H. Guo, and J. Wang, Phys. Rev. B **63**, 245407 (2001).
[16] M. Brandbyge, J.-L. Mozos, P. Ordejón, J. Taylor, and K. Stokbro, Phys. Rev. B **65**, 165401 (2002).
[17] QuantumWise HP, http://www.quantumwise.com/
[18] N. Troullier and J. L. Martins, Phys. Rev. B **43**, 1993 (1991).
[19] J. P. Perdew and A. Zunger, Phys. Rev. B **23**, 5048 (1981).
[20] There is a big difference between the calculated and experimental (0.95 ± 0.11 V[4]) values of V_{infl}. In this study, we took the HOMO level as the resonant state responsible for tunneling currents. If we take the state originating from the LUMO level by the opposite biases, the calculated value would be about 1.4 V because the resonant LUMO state is positioned at around 1.4 eV above the metal Fermi energy in our calculations. However, the difference remains large. One of the reasons is the poorness of the local-density approximation for the DFT calculations on the metal-molecule contacts. The gap would be close if we use the GW approximation (Ref. 9) and/or the self-interaction correction.